Energy & Buildings 357 (2026) 117124

Contents lists available at ScienceDirect

Energy & Buildings

journal homepage: www.elsevier.com/locate/enb

A novel hydroponic roof system for the energy renovation of flat roofs in the Mediterranean area[☆]

V. Costanzo [a,*], M. Detommaso [a], G. Evola [a], F. Nocera [b], M. Mistretta [c], S. Longo [d]

[a] Department of Electrical Electronic and Computer Engineering (DIEEI), University of Catania, Via S. Sofia 64, 95123 Catania, Italy
[b] Department of Civil Engineering and Architecture (DICAr), University of Catania, Via S. Sofia 64, 95123 Catania, Italy
[c] Department of Information Engineering, Infrastructure and Sustainable Energy University Mediterranean of Reggio Calabria, Via Graziella, Feo di Vito, 89122 Reggio Calabria, Italy
[d] Department of Engineering, University of Palermo, Viale delle Scienze Bld. 9, 90128 Palermo, Italy

ARTICLE INFO

Keywords:
Hydroponic roof
Indoor temperature
Energy savings
Experimental campaign
TRNSYS

ABSTRACT

This study introduces and validates a novel Deep Water Culture hydroponic roof system as a building-integrated solution for enhancing indoor thermal conditions and energy efficiency in Mediterranean climates. Unlike conventional green roofs, the proposed system removes the soil layer and uses a water-based nutrient solution that simultaneously supports plant growth and acts as a thermal energy buffer. A full-scale prototype was experimentally tested on an existing office building in Catania (Italy); based on the experimental data, transient thermal modelling is then undertaken with TRNSYS to simulate the prototype with different roof configurations.

Results show that the hydroponic roof reduces indoor peak temperatures by up to 2.8 °C in the summer, increases them by 2.4 °C in the winter and shifts heat flux peaks by up to 16 h. Annual simulations indicate energy savings of 47% for space cooling and 51% for space heating, too. The DWC hydroponic roof demonstrates strong potential as a relatively lightweight, passive retrofit technology combining urban agriculture and building decarbonization.

1. Introduction

The building sector is known to be responsible for a big amount of global energy consumption and carbon dioxide emissions [1]. Currently, the increase of the outdoor air temperature worldwide and the more frequent heat wave events are inducing a higher demand of energy for space cooling to maintain comfortable indoor thermal conditions [2]. In this light, the adoption of measures for reducing the energy consumption while decarbonizing the building sector represents one of the main objectives of the European Union action [3].

In the last decade, several studies dealt with the investigation of the thermal performances of some innovative green constructions and their effectiveness in the reduction of the energy consumption of buildings [4], with a particular focus on green roofs and green facades [5–7]. Such studies highlighted the ability of vegetation-based systems to mitigate the Urban Heat Island (UHI) phenomenon, improve outdoor thermal comfort and decrease the buildings energy demand for cooling thanks to the combined effect of shading and evapotranspiration of the foliage layer [8].

Despite these benefits, conventional green roofs also present some limitations, mainly related to the physical characteristics of the growing substrate, which plays the crucial in determining the overall thermal performance [9]. Although the presence of organic matter improves the soil properties for plant growth, excessive organic content can promote weed proliferation and water contamination during runoff [10]. Moreover, the thermo-physical properties of the substrate such as thermal conductivity, density, specific heat, and thermal emissivity vary with soil moisture content, significantly affecting the roof energy balance [11].

To overcome these issues, Building Integrated Agriculture (BIA) has recently emerged as a promising approach that integrates soilless plant cultivation technologies within buildings to enhance both resource efficiency and environmental performance [12]. BIA leverages the synergies between buildings and agriculture, enabling the recovery of water, energy and nutrients from internal flows [13]. Within this framework, hydroponic roof systems represent an advanced alternative to traditional green roofs, offering reduced water and soil consumption,

☆ This article is part of a special issue entitled: 'ENB_Ecological Buildings' published in Energy & Buildings.

* Corresponding author.
E-mail address: vincenzo.costanzo@unict.it (V. Costanzo).

https://doi.org/10.1016/j.enbuild.2026.117124
Received 14 November 2025; Received in revised form 19 January 2026; Accepted 5 February 2026
Available online 6 February 2026

Nomenclature

Greek letters

α	Solar absorptance, –
Θ	Water content, –
ε	Emissivity, –
λ	Thermal conductivity, W/(m•K)
ρ	Density, kg/m^3

Symbols

CE	Thermal energy demand for space cooling per unit surface, kWh/(m^2•y)
CES	Cooling energy savings, %
c	Specific heat, J/(kg•K)
G	Global solar irradiance, W/m^2
HE	Thermal energy demand for space heating per unit surface, kWh/(m^2•y)
HES	Heating energy savings, %
MAE	Mean Absolute Error, °C
r	Pearson's coefficient, –
R	Coefficient of determination, –
RH	Relative humidity, %
RMSE	Root Mean Square Error, °C
q	Heat flux, W/•m^2
SM	Surface mass, kg/•m^2
T	Temperature, °C
t	Thickness or depth, m
U	Thermal transmittance W/(m^2•K)
X	Fraction of covered surface, –
Y	Periodic thermal transmittance W/(m^2•K)
w	Wind speed, m/s

Subscript

i	initial
int	internal air
p	constant pressure
peak	peak value
o	outdoor
os	outer surface
s	sky
veg	vegetation
w	water in the hydroponic tank

optimized nutrient management and the elimination of problems related to substrate degradation [13,14].

In hydroponic systems, plant cultivation takes place in a nutrient solution dissolved in water, thus overcoming the thermal variability and maintenance issues of soil-based systems [15]. Among the various configurations, the DWC system has a typical thickness lower than 50 cm for horizontal layouts and is particularly suitable for building applications due to its simplicity, adaptability and the possibility to host a wide variety of plant species from edible crops to ornamental plants [16].

However, the literature concerning the thermal and energy performance of hydroponic roofs remains very limited [9]. Most existing studies have focused on experimental measurements of external surface temperature and heat flux through the roof in presence of a hydroponic module in hot and dry or subtropical climates [9]. For instance, Huang et al. compared the performance of hydroponic and conventional green roofs in Taichung (Taiwan) and observed reductions of up to 11 °C in rooftop surface temperature and 60% in heat flux amplitude [17]. Alexandri and Jones examined the effects of several passive cooling techniques such as reflective coatings, vegetated roofs and hydroponic modules across different climatic conditions, reporting temperature reductions up to 15 °C for hydroponic systems [18]. Similarly, Tanaka et al. measured air, water and surface temperatures on an experimental setup in Osaka (Japan), confirming the potential of hydroponic roofs to mitigate rooftop overheating [19].

Only a few studies have adopted numerical modelling to estimate the annual energy savings achievable with hydroponic roofs [9]. Ibrahim et al. [20], using a simulation approach for a 15 cm-deep water layer in Alexandria (Egypt), reported potential reductions of 14% in cooling and 10% in heating energy demand compared to a bare roof. Despite these promising results, there is still a lack of studies combining experimental measurements and validated dynamic simulations to assess the full-year thermal behaviour of hydroponic roofs, especially under Mediterranean climate conditions.

The present study aims to fill this gap by developing and experimentally validating a dynamic TRNSYS model of a modular DWC hydroponic roof prototype designed within the Italian PRIN research project FUD-OF-SITHY ("Favor the Urban Development OF Sustainable agriculture Through Hydroponics"). The validated model is then used to analyse, under both free-running and controlled (i.e., thermostatic) conditions, the impact of the hydroponic system on indoor thermal conditions, heat flux attenuation and building energy demand in various roof configurations. This work provides new quantitative evidence on the dual role of hydroponic roofs as energy-saving and climate-adaptive technologies, supporting their application in the energy retrofit of existing buildings.

The novelty of the approach adopted can be summarised as follows: i) new modular design for a DWC system tested with a long-term experimental campaign in a Mediterranean climate (no previous studies were found for such climate zone); ii) validation of a TRNSYS model for the transient modelling of the hydroponic system; iii) scenario analysis to deeply investigate the role of water depth, thermal mass, and the influence of the vegetation fraction covering the roof surface in different roof configurations and under both free-running and thermostatic conditions.

2. Materials and methods

2.1. Framework of the methodology

The investigation described in this paper is framed upon the following phases, as detailed in Fig. 1:

1. Construction of an experimental mock-up of a novel Deep-Water Culture (DWC) hydroponic module
2. Measurement of the water temperature and of the external roof surface temperature.
3. Creation of a transient thermal model of a sample office room below the DWC module in TRNSYS.
4. Use of local weather data and of the experimental measurements for validating the TRNSYS model.
5. Detailed modelling of the sample room under three different configurations for the building envelope, both with and without the DWC module.
6. Comparative analysis of indoor air temperature in free running mode and of the energy demand for space heating and cooling under thermostatic control.
7. Sensitivity analysis of different water depths and roof surface fractions covered by the vegetation.

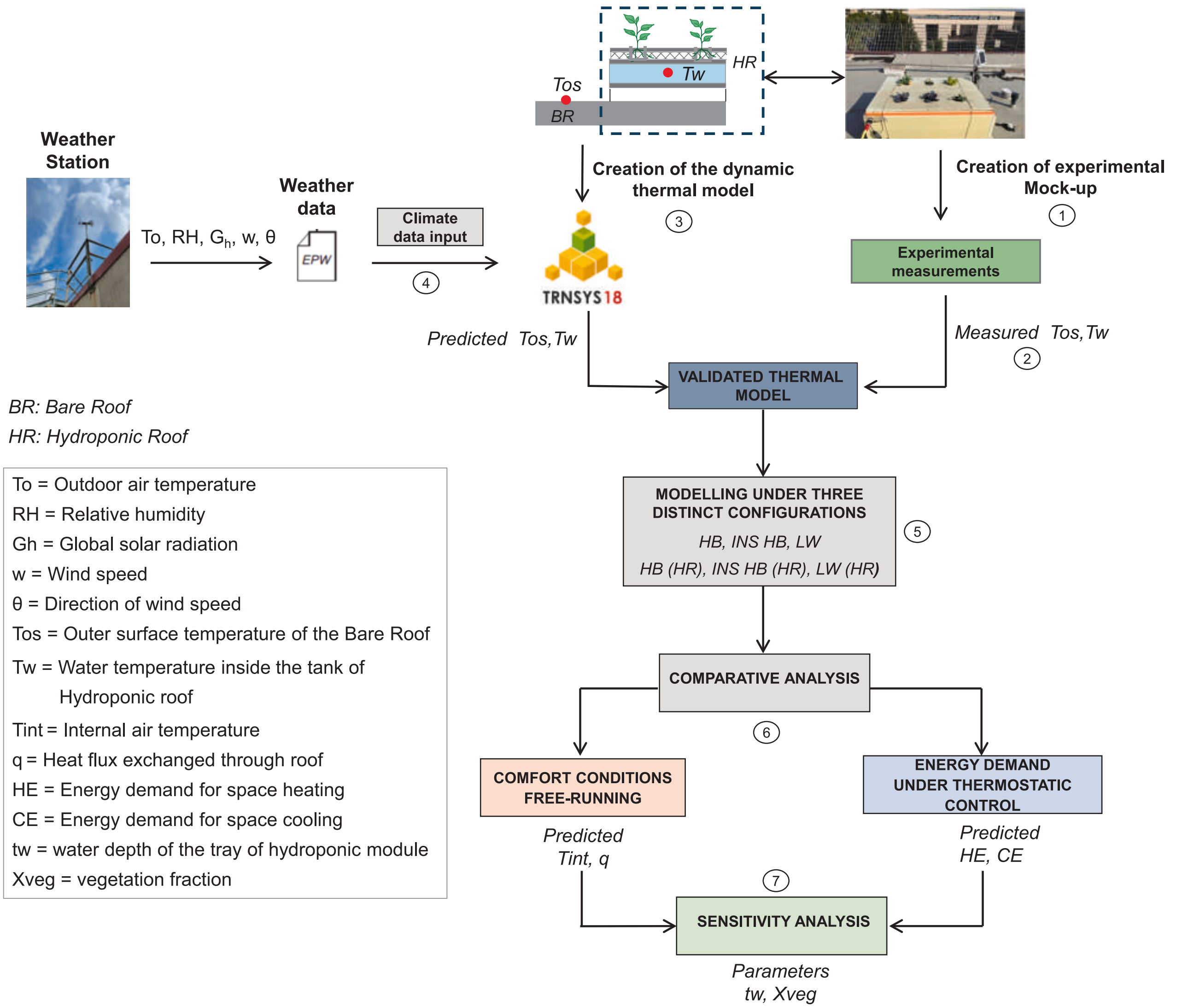

Fig. 1. Workflow of the research methodology.

2.2. Description of the experimental setup

The prototype of the hydroponic module was installed on the flat roof of an existing building at the Civil Engineering Department of the University Campus of Catania (Latitude 37°30′ N, Longitude 15°04′ E). The city of Catania, located in Southern Italy, is characterized by a mild climate, classified as Csa according to the Köppen-Geiger climate classification.

The building where the hydroponic module is installed has three floors above the ground and hosts some classrooms in the first and second floors, respectively, and a series of cellular offices in the top floor. The experimental setup was placed on the flat roof of an office room with a south-facing external wall. Fig. 2a and 2b show two aerial views of the University Campus that include the case study building and the nearest weather station used for gathering weather data, whereas Fig. 2c shows the experimental setup and Fig. 2d details the materials that make up the hydroponic module (HR) and the existing bare roof (BR).

The existing bare roof (BR) is made of 16-cm hollow clay blocks and 6-cm reinforced concrete slab on top of which the lightweight concrete screed and the clay tiles are placed.

The innovative DWC hydroponic system is composed of a plastic tank of 124 x 85 cm^2 with a height of 35 cm and a volume of 240 L. The tank is raised from the existing bare roof by means of a wood support that creates a lightly ventilated horizontal air gap of about 4 cm. A 5-cm layer of extruded polystyrene makes up the thermal insulation of the module both on the vertical sides and on the bottom, while the top hosts a 3-cm perforated polystyrene board that includes six mesh pots with the crops to grow. Thereby, the roots of the seedings are soaked in an oxygenated nutrient solution.

The module is also equipped with a recirculation pump of 300 L/h flow rate, a water reintegration system and an oxygenator: the pump is used to allow the movement of the water and nourishment of the plants, while the oxygenator is used to deliver pure oxygen to the roots. Both pumps and oxygenator have constant electric absorption of 5 W during their operation, which is triggered by an automatic Wi-Fi cyclic timer twice in the morning (from 6:00 to 7:00 and from 11:00 to 12:00), in the afternoon/evening (from 15:00 to 16:00 and from 19:00 to 20:00) and in the night (from 23:00 to 24:00 and from 3:00 to 4:00). The resulting electricity consumption is thus very low (30 Wh per day, i.e. around 11 kWh per year) and is not accounted for hereafter in the energy analyses.

Fig. 3 depicts the various components of the experimental setup including the water tray, the oxygenator, the recirculation pump, the measurements node with its sensors and probes, and a wireless/LAN IP Gateway.

Lettuce (*lactuca sativa*) and basil (*ocimum basilicum*) plant species have been first cultivated in the hydroponic module. These plants were chosen due to their fast growth cycle, high adaptability to hydroponic

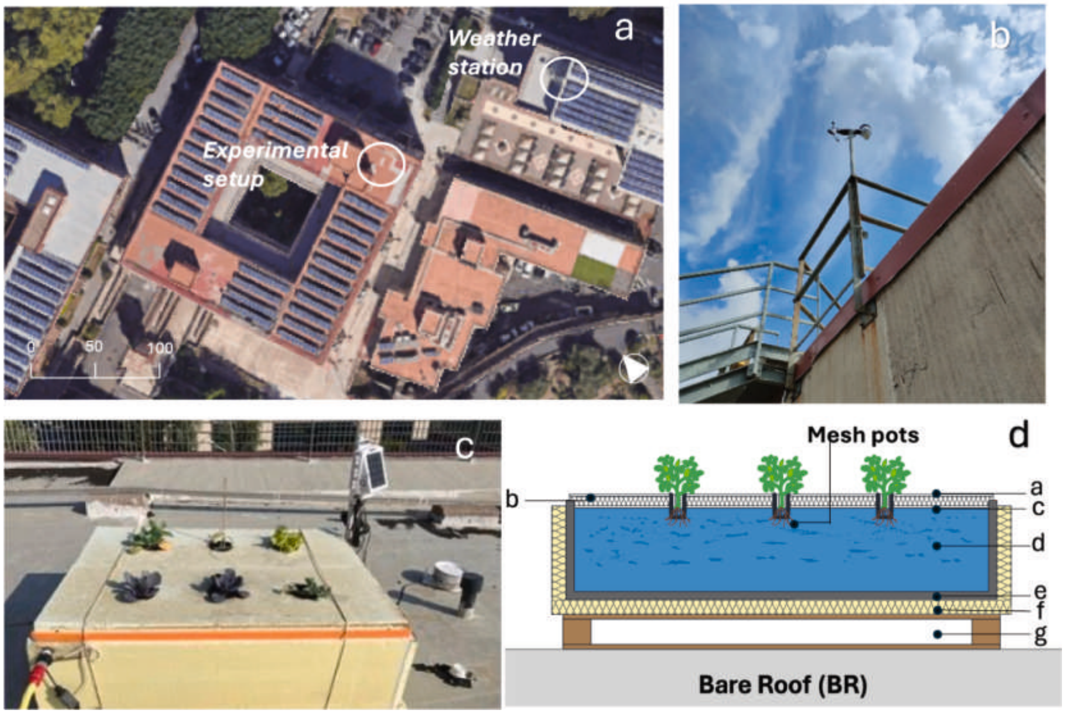

Fig. 2. DWC hydroponic roof prototype: a) Aerial view of the installation site; b) Stationary weather station; c) Detailed view of the experimental mock-up; d) Vertical section of the mock-up with the various materials.

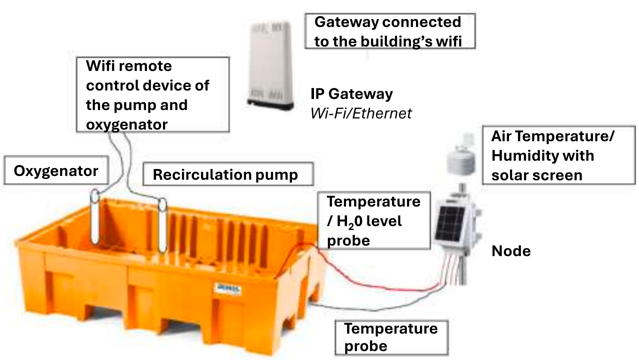

Fig. 3. Experimental apparatus of the hydroponic module.

systems and to local weather conditions, making them suitable for evaluating the thermal and agronomic performance of the hydroponic roof module. Both plant species have shallow root systems, which allows them to efficiently absorb nutrients from the oxygenated water solution while requiring minimal maintenance.

The thermo-physical features such as thickness (t), thermal conductivity (λ), density (ρ), and specific heat (C_p) of all layers (a-g) of the hydroponic roof module (HR) are reported in Table 1.

The thermal features of the polycarbonate lid shell (layers *a* and *c*) and extruded polystyrene (layer *b*) are certified by the manufacturer according to the Italian standard UNI 10456:2008 [21] and UNI 10351:2021 [22]. The equivalent thermal conductivity of the air gap is instead evaluated based on the thermal resistance of a lightly horizontal ventilated air gap according to UNI EN 6946:2018 Standard [23]. The hydroponic module thus results in a total thickness of 44 cm, a U-value = 0.35 W/(m^2·K), a dynamic thermal transmittance value Y_{ie} = 0.001 W/(m^2·K) and surface mass SM = 307 kg/m^2.

Table 1
Layers and thermal features of the hydroponic module.

	Layer	t (cm)	λ (W/(m·K))	ρ (kg/m^3)	Cp(J/(kg·K))
a	Polycarbonate top lid shell	1.0	0.20	1200	1200
b	Extruded polystyrene	3.0	0.032	33	1450
c	Polycarbonate bottom lid shell	1.0	0.20	1200	1200
d	Water solution	30.0	0.56	1000	4186
e	Polycarbonate floor	0.3	0.20	1200	1200
f	Extruded polystyrene	5.0	0.032	33	1450
g	Slightly ventilated air gap	4.0	0.20	1.2	1000

2.3. Weather data and experimental measurements campaign

The experimental setup comprises a wireless stationary weather station and a wireless portable station equipped with temperature probes. The wireless stationary weather station, placed on top of a building in front of the experimental site (see Fig. 2b), was used to collect the weather data required for the simulations in TRNSYS every 15 min: it measured air temperature, relative humidity, wind speed and direction, and precipitation. The accuracy, resolution, and measurements range of the relative sensors are reported in Table 2.

Global, direct and diffuse solar irradiance values were instead collected from the weather station of the "Sicilian Agro-meteorological Informative Service" (SIAS), placed in the immediate surroundings of the University Campus of Catania. Fig. 4 reports the weather data, such as air temperature, relative humidity, global solar radiation and wind speed, for the entire experimental period, i.e., from 25 June to 25 October 2024, which has been used for validation purposes. Instead, annual simulations relied on a Typical Weather Year (TWY) file created by the authors based on recent local weather observations [24].

Finally, the water temperature within the hydroponic module and the external surface temperature of the existing bare roof have been collected by means of a wireless portable station. This instrumentation was equipped with a wireless multi-functional probe for measuring water depth, temperature and electrical conductivity in the tray (Water depth: range = 0–11 m, accuracy ± 0.05%; Temperature: resolution = 0.01 °C, accuracy = ± 0.1 °C; electrical conductivity: range = 5–100000 μS/cm, resolution = 0.1 μS), and a Pt 100 probe to measure the surface temperature on the bare roof (resolution = 0.1 °C, accuracy = ± 0.1 °C). These temperature data were collected with a sample time of 15 min and transmitted remotely through a wireless/LAN IP Gateway to a server collecting all the data coming also from the stationary weather station.

2.4. Features of the TRNSYS model, validation procedure, and simulation outputs

The sample room with the existing bare roof and the experimental hydroponic module has been modelled in TRNSYS environment. For the sake of modelling the scenarios with the hydroponic module, the green roof component (Type 785 initially developed by Hong et al. [25]) has been used by modifying various input parameters and then coupled with Type 56 ("multi-zone building model"). Fig. 5 represents the flowchart for coupling the multizone building model (Type 56) to the green roof component (Type 785) in TRNSYS simulation studio.

More in detail, the simulation workflow includes the following phases according to the numbers reported in Fig. 5:

1. Implementation of the local weather data through Type 15–3.
2. Building modelling and settings in Type 56, e.g., definition of the thermal features of the sample room and its boundary conditions.
3. Energy balance on the building model with the bare roof (Type 56).
4. Implementation of input data in the green roof component (Type 785) as feedback from the bare roof of Type 56 (TRNbuild output).
5. Implementation of local weather and precipitation data in the green roof component (Type 785).
6. Implementation of the modified modelling inputs in the green roof component (Type 785).
7. Energy balance of the green roof component (Type 785).
8. Calculation of requested outputs under free-running conditions (Indoor air temperature values, heat flux through the roof).
9. Calculation of the energy demand for space heating and cooling under thermostatic control.

As anticipated, some input parameters of the green roof component (Type 785) have been modified to model the hydroponic system. In particular, the soil layer has been treated as a homogeneous water layer with a water content equal to 100% all over the simulated period to consider that the potential amount of water evaporated is continuously replaced by a re-filling. Then, the surface radiative and optical properties of the soil have been modified to reflect those of the polycarbonate top lid shell layer, which is the actual covering material of the tank. As for the vegetation layer, the radiative properties, solar absorptivity (α_{veg}) and thermal emissivity (ε_{veg}) of the leaves have been taken from Ref. [26], while its fraction (X_{veg}) has been calculated considering the horizontal projected area of the leaves under full development conditions. The initial water temperature within the tank ($T_{w,i}$) was instead set at the same value measured in the water tray at the beginning of the experimental campaign. The main input parameters of the hydroponic roof model are summarized in Table 3.

In the "Multi-zone building model" (Type 56), a sample room with intended office use has been modelled. The room has a gross volume of 24.3 m^3, a gross height of 2.70 m and a net floor area of 9.0 m^2. All walls are adjacent to other rooms with the same thermal conditions (adiabatic surfaces), except for the south-facing wall that hosts a window with external surface of 1.2 m^2. The external wall is made of alveolate clay blocks without thermal insulation (U_{wall} = 0.50 W/(m^2·K)), the roof is a flat reinforced concrete slab with hollow clay blocks (U_{roof} = 1.57 W/(m^2·K)), while the window is a typical double-glazing with air gap (U_{window} = 2.80 (W/m^2·K)). The solar absorptivity (α_{os}) and thermal emissivity (ε_{os}) of the external roof surface have been set to 0.7 and 0.9, respectively. Moreover, the air infiltration rate was set at the constant value of 0.5 h^{-1} throughout the day, while internal gains follow the typical schedule of offices: the room is used from 8:00 to 18:00 during workdays with a density of 0.1 people/m^2, each releasing 118 W of sensible heat. The power density of equipment and lighting were set to 6.0 W/m^2 and 4.0 W/m^2 respectively.

The validation of the model has been carried out in free-running conditions, i.e., without any heating and cooling systems in operation, by comparing the experimental and simulated values of both the external surface temperature of the bare roof (T_{os}) and the water temperature (T_w) inside the hydroponic module. To this purpose, statistical indexes such as the Error percentage, Mean Absolute Error (MAE), Root Mean Square Error (RMSE), Pearson's coefficient (r) and the coefficient of determination (R^2) quantify the discrepancies between measured and predicted data. Based on the validated model, the indoor air temperature (T_{int}), the heat flux exchanged from the internal surface of the roof (q), and the annual heating and cooling energy demand (excluding the very low energy required for the recirculation pump and oxygenator), have been requested as an output in all the investigated configurations. In particular, daily trends of T_{int} and q have been analysed in detail during a typical hot summer week and a cold winter week, while the energy demand for heating and cooling has been appraised by simulating a thermostatic control switched on during workdays from 8:00 to 18:00. In the case of space heating, the energy demand has been calculated from 1st December to 31st March using a set-point temperature of 20 °C, while for space cooling the energy demand has been calculated from 1st June to 30th September with a set-point temperature of 26 °C.

2.5. Scenario analysis

For the sake of assessing the thermal performance of the novel DWC hydroponic system, three different building envelope scenarios have been considered:

- Scenario *HB:* external walls are made of alveolate clay blocks (*W_HB*) while the roof is realized with a reinforced concrete slab and hollow clay blocks (*R_HB*). This scenario represents the actual constructive configuration of the sample room.
- Scenario *INS_HB:* the same as Scenario HB but with the addition of a thermal insulation layer in both the external walls and the roof to comply with the current Italian building codes.
- Scenario *LW:* both external walls and the roof are made of insulated lightweight sandwich panels. This scenario explores the use of the hydroponic system in well-insulated lightweight structures.

Table 2
Sensors features of the stationary weather station.

Sensor	Accuracy	Resolution	Measurement range
Air Temperature	± 0.3 °C	0.1 °C	−40 ÷ 60 °C
Relative Humidity	± 2%	1%	1 ÷ 100%
Anemometer – wind speed	± 0.9 m/s	0.4 m/s	0 ÷ 89 m/s
wind direction	± 3°	1°	1 ÷ 360°
Rain gauge	± 5% up to 250 mm/hr	0.1 mm/hr	1 ÷ 762 mm/hr

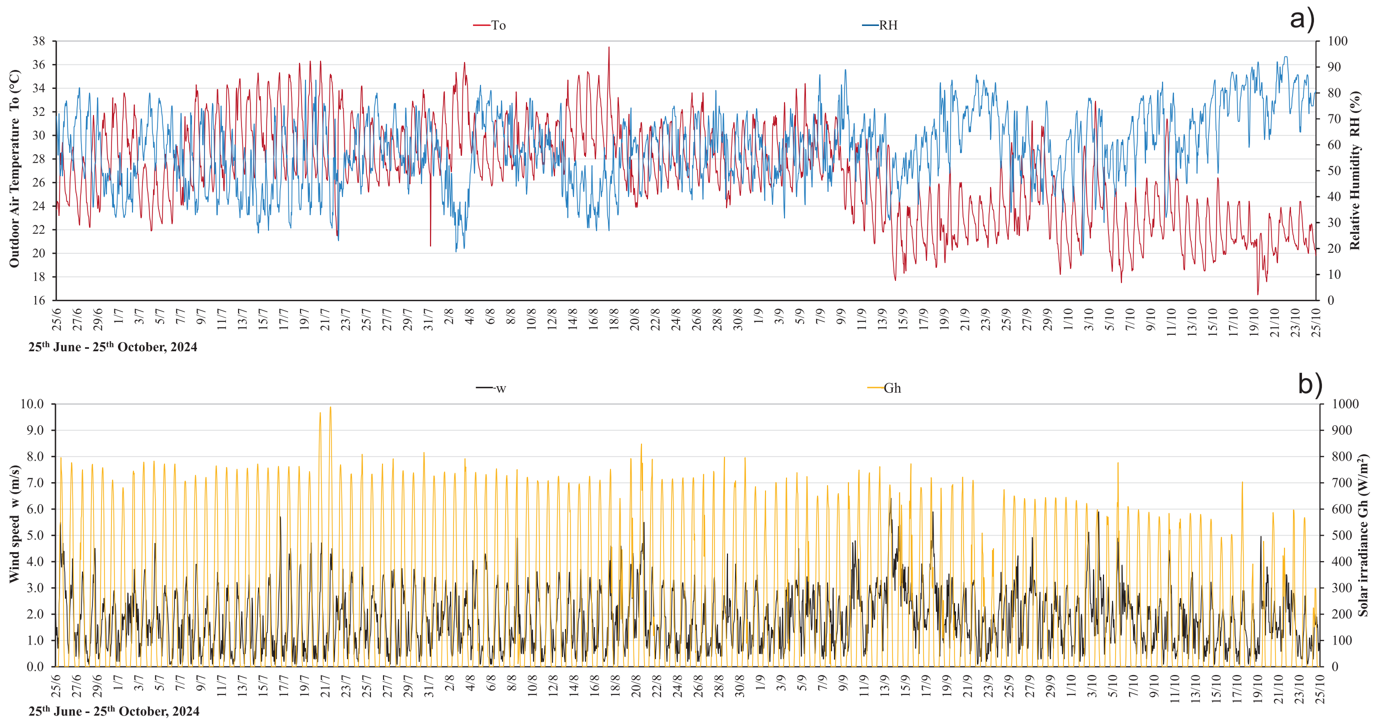

Fig. 4. Weather data recorded by the stationary weather station from 25th June to 25th October 2024. a) Temperature and relative humidity; b) Global solar radiation and wind velocity.

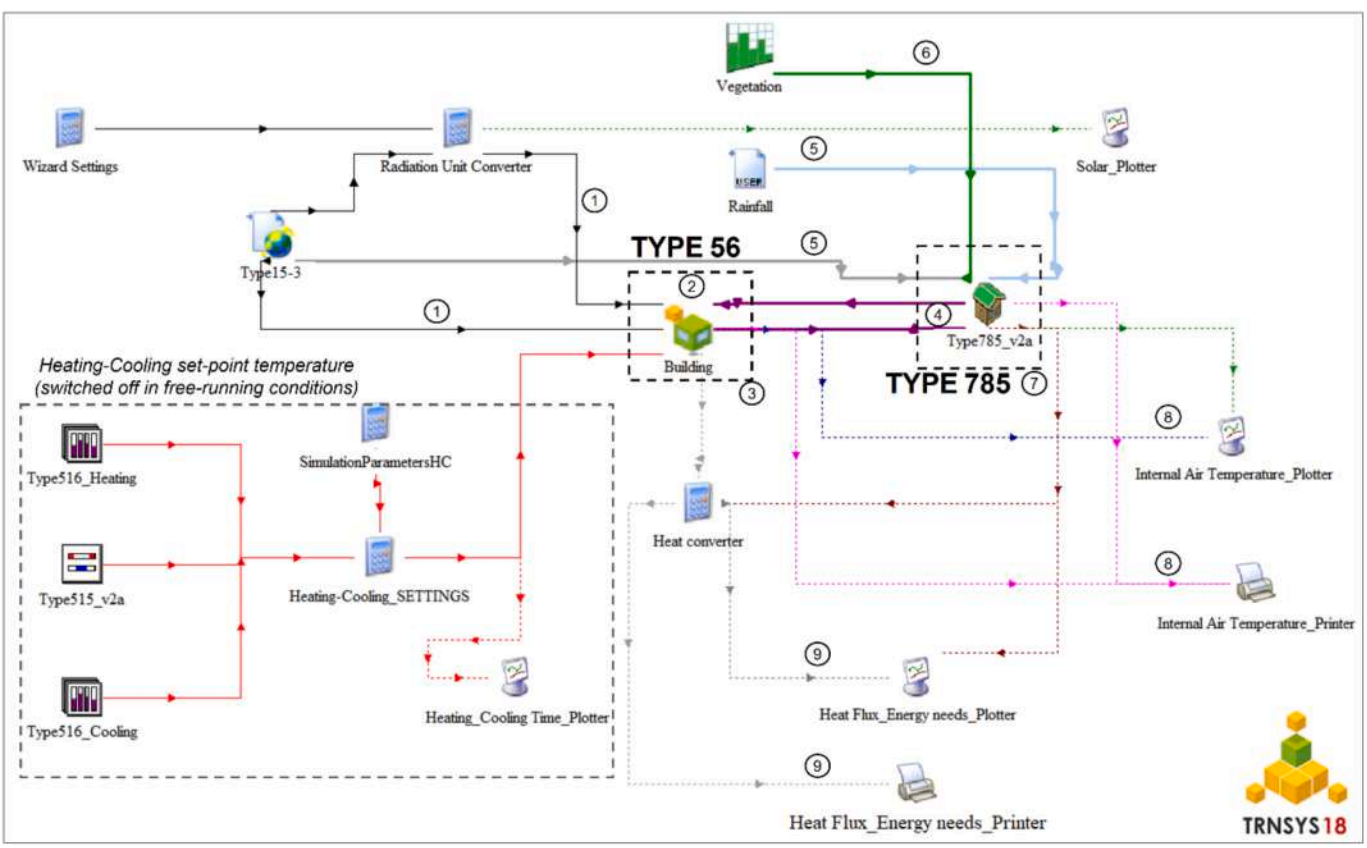

Fig. 5. TRNSYS simulation workflow.

Table 3
Input parameters required by TRNSYS Type 785 for modelling the Hydroponic module.

Parameters	Name		Value
Vegetation fraction	X_{veg}	–	0.15
Vegetation absorptivity	α_{veg}	–	0.60
Vegetation emissivity	ε_{veg}	–	0.97
Solar absorptivity of the top lid	α_{os}	–	0.40
Emissivity of the top lid	ε_{os}	–	0.90
Depth of the water layer	t_w	m	0.30
Thermal conductivity of water	λ_w	W/(m•K)	0.60
Density of water	ρ_w	Kg/m^3	1000
Specific heat of water	C_{pw}	J/(kg•K)	4186
Bare roof U-value	U	W/(m^2•K)	1.57
Initial water content	$\Theta_{w,i}$	–	100%
Initial water temperature	$T_{w,i}$	°C	14.8

The various layers of materials and their thermal properties such as thickness (t), thermal conductivity (λ), specific heat (C_p) and density (ρ) of all the investigated scenarios are reported in Table 4. Table 5 summarizes the resulting stationary thermal transmittance (U), dynamic thermal transmittance (Y_{ie}), surface mass (SM) and total thickness (t) values for the investigated scenarios with and without the hydroponic module, whereas Table 6 reports the steady state and dynamic parameters of the walls analysed.

3. Results and discussion

3.1. Validation of the thermal model

The validation of the TRNSYS model has been carried out based on the hourly values of external roof surface temperature and water temperature within the hydroponic module recorded from 25^h June to 25th October 2024. Fig. 6 reports the comparison between the measured and simulated values for both these temperatures and shows an excellent agreement between measured data (solid grey lines) and simulated data (dashed grey lines) for the bare roof (BR) throughout all the four months (Fig. 6a). As regards the water temperature, the observed and simulated values are in very close agreement too (Fig. 6b), and this is rebated by the calculation of the statistical indices introduced in Section 2.7: for T_{os} the percentage error is 6%, MAE is 1.75 °C and RMSE is 2.40 °C, while for T_w the percentage error is 5%, MAE is 1.14 °C and RMSE is 1.37 °C, respectively.

For both the BR and HR configurations, a good correlation is confirmed by the very high values of the Pearson's coefficient. i.e., r = 0.97 and r = 0.98 in order, and by regression lines whose coefficients of determination are always $R^2 > 0.90$ (Fig. 7).

3.2. Thermal analysis of the indoor environment

This section discusses the results of the dynamic thermal simulations carried out in free-running conditions for the three investigated configurations both with and without the inclusion of the DWC hydroponic roof module. The analysis is focused on the hourly variations of the indoor air temperature (T_{int}) during both a typical summer week (from 9 July to 16 July, see Fig. 8) and winter week (from 22 January to 29 January, see Fig. 9) in Catania.

In the summer week, the insulated lightweight configuration (*LW*) shows the highest fluctuations, with peak temperatures of around 39 °C and minimum temperatures of about 31 °C (see Fig. 8a). As regards scenario *HB* (uninsulated roof made of hollow clay blocks), lower daily indoor temperature fluctuations are predicted due to the higher thermal mass than the lightweight configuration (*LW*). Indeed, for this configuration, T_{int} oscillates between a minimum of 31.9 °C and a maximum of 35.8 °C, showing peak values significantly dampened and delayed if compared to the lightweight scenario (*LW*). The *INS_HB* configuration presents the most stable profile of internal air temperature thanks to the high level of thermal insulation of the roof slab. In fact, for this case the daily fluctuations are within 3.0 °C during the selected summer week (see Fig. 8a).

Fig. 8b provides additional valuable insights about the indoor thermal conditions under the effect of the hydroponic roof module during the summer: in fact, the inclusion of a hydroponic roof module in a lightweight roof (*LW_HR*) contributes to dampen the daily fluctuations of the indoor temperature, which now varies from 30.3 °C to 37.7 °C. In presence of the hydroponic module, the roof with hollow clay blocks without thermal insulation (*HB_HR*) and with thermal insulation (*INS_HB_HR*) show the maximum peak value of T_{int} of 33.4 °C and 33.9 °C, respectively. In a typical winter week (22nd – 29th January), the LW configuration shows the widest daily fluctuation, with a peak value of 16.4 °C and a minimum value slightly below 10 °C. On the contrary, *HB* and *INS_HB* configurations present the flattest profile with an amplitude of daily fluctuation below 2.2 °C. *INS_HB* scenario is also

Table 4
Layers and thermal properties of the construction materials for the different scenarios [22].

Scenario	Component	No	Layers	t (cm)	λ(W/(m·K))	ρ (kg/m^3)	C_p(J/(kg·K))
HB		1	Clay tiles (outer layer)	2.0	1.50	1500	1000
		2	Lightweight concrete	4.0	1.00	1400	1200
	Roof (*R_HB*)	3	Waterproofing membrane	0.2	0.20	1000	1200
		4	Hollow clay blocks + concrete slab	22.0	0.56	1280	1000
		5	Lime and cement mortar (inner layer)	3.0	0.90	1000	1000
		1	Lime and cement mortar (outer layer)	3.0	0.90	1800	1000
	Wall (*W_HB*)	2	Alveolate clay block (Poroton 850)	30.0	0.18	850	1000
		3	Lime and cement mortar (inner layer)	3.0	0.90	1800	1000
		1	Clay tiles (outer layer)	2.0	1.50	1500	1000
		2	Lightweight concrete	4.0	1.00	1400	1200
	Roof (*R_INS_HB*)	3	Waterproofing membrane	0.2	0.20	1000	1200
		4	Extruded polystyrene layer	8.0	0.034	15	1450
		5	Bitumen layer	0.2	0.17	1200	1000
HB_INS		6	Hollow clay blocks + concrete slab	22.0	0.56	1280	1000
		7	Lime and cement mortar (inner layer)	3.0	0.90	1800	1000
		1	Lime and cement mortar (outer layer)	3.0	0.90	1800	1000
		2	Polystyrene layer	5.0	0.04	15	1450
	Wall	3	Cement mortar	1.0	1.40	1800	1000
	(*W_INS_HB*)	4	Alveolate clay block (Poroton 850)	30.0	0.18	850	1000
		5	Lime and cement mortar (inner layer)	3.0	0.90	1800	1000
	Roof (*R_LW*)Wall	1	OSB panel (outer layer)	0.9	0.12	650	1700
LW	(*W_LW*)	2	Polystyrene layer	6.5	0.04	15	1450
		3	OSB panel (Inner layer)	0.6	0.12	650	1700

Table 5
Steady-state and dynamic thermal parameters for the roof with and without the hydroponic module.

No	Investigated scenarios	Roof without hydroponic module	Cross section	Thermal features	Investigated scenarios	Roof with hydroponic module	Thermal features
I	HB	R_HB	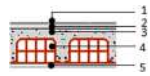	t = 31 cm U = 1.57 W/(m^2·K) Yie = 0.68 W/(m^2·K) SM = 367 kg/m^2	HB_HR	R_HB_HR	t = 75 cm U = 0.31 W/(m^2·K) Yie = 0.001 W/(m^2·K) SM = 671 kg/m^2
II	INS_HB	R_INS_HB	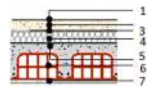	t = 39 cm U = 0.34 W/(m^2·K) Yie = 0.059 W/(m^{2}K) SM = 422 kg/m^2	INS_HB_HR	R_INS_HB_HR	t = 83 cm U = 0.19 W/(m^2·K) Yie = 0.001 W/(m^2·K) SM = 705 kg/m^2
III	LW	R_LW	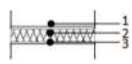	t = 8 cm U = 0.52 W/(m^2·K) Yie = 0.51 W/(m^2·K) SM = 15 kg/m^2	LW_HR	R_LW_HR	t = 52 cm U = 0.22 W/(m^2·K) Yie = 0.01 W/(m^2\K) SM = 313 kg/m^2

Table 6
Resulting stationary and dynamic thermal parameters for the different wall configurations in the investigated scenarios.

No	Investigated scenarios	Wall	Cross section	Thermal features
I	HB / HB_HR	W_HB	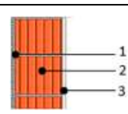	t = 36 cm U = 0.52 W/(m^2·K) Yie = 0.068 W/(m^2·K) SM = 255 kg/m^2
II	INS_HB / INS_HB_HR	W_INS_HB	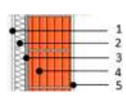	t = 42 cm U = 0.31 W/(m^2·K) Yie = 0.012 W/(m^2·K) SM = 260 kg/m^2
III	LW / LW_HR	W_LW	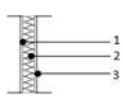	t = 8 cm U = 0.52 W/(m^2·K) Yie = 0.51 W/(m^2·K) SM = 15 kg/m^2

characterized by the highest value of indoor air temperature, with a peak of 15.8 °C (see Fig. 9a). A closer analysis of these hourly trends suggests that the DWC hydroponic module contributes to increase the thermal insulation of the roofs, thus keeping higher indoor air temperatures compared to bare roof configurations (Fig. 9b).

Moreover, the reduction in the peak value of indoor air temperature was evaluated for the summer day where the highest peak values were found for all investigated roof typologies, namely the 13rd of July. In the winter, the 25th January was selected as it is characterized by the lowest daily minimum indoor temperatures in the investigated winter week. Table 7 thus reports the minimum and maximum values of indoor air temperature predicted on such days, along with the differences between the corresponding values for the bare roof (*BR*) and the hydroponic roof (*HR*) configurations.

In the hottest summer day, the peak of indoor air temperature can be reduced by 2.4 °C and 1.7 °C in the uninsulated concrete roof (*HB*) and prefabricated lightweight roof (*LW*) when the hydroponic module is added. A reduction of 1.3 °C for the concrete roof with high thermal insulation level (*INS_HB*) was also found. As regards the indoor thermal conditions in winter, the insulating effect provided by the hydroponic roof is marked in the *HB_HR* configuration, where an increase in the maximum indoor air temperature value of 2.1 °C was achieved on January 25th (see Table 7). In the roof configuration with a high level of thermal insulation (*INS_HB*), the addition of a DWC hydroponic system allows increasing the peak air temperature of about 1.0 °C. On the contrary, the presence of a DWC module in the lightweight configuration (*LW*) involves a reduction of 0.5 °C in the sunny hours because of the heat stored by the water. Overall, the results revealed that the inclusion of a hydroponic module is more effective under those roof configurations that present no or low thermal insulation.

3.3. Energy analysis

The analysis of the heat flux transferred through the roof is crucial to assess the energy balance of the different scenarios, given the major role played by solar irradiance. Fig. 10 represents the daily profile of the heat flux for each investigated scenario in the bare roof configuration and with the addition of the hydroponic roof module during a typical summer week, while Fig. 11 refers to a winter week. Table 8 reports the peak value of the heat flux and the time when the peak value is achieved, thus providing insights about the thermal buffering capacity of the different solutions.

The analysis of the time trend of the incoming heat flux through the roof during the summer week highlights that the lightweight roof configuration (*LW*) experiences notable fluctuations, with the predicted peak value of about 10.4 W/m^2 in phase with the maximum solar irradiance at 13:00, as depicted in Fig. 10a. This indicates also an almost instantaneous response to external forcing conditions due to the very low thermal mass of this configuration. The scenario *HB* shows the widest fluctuations due to the higher U-value of the roof compared to the other two configurations (*LW, INS_HB*). In this case, the peak value of 11.7 W/m^2 occurs at 21:00 (Fig. 10a). On the contrary, the configuration *INS_HB* presents the narrowest fluctuations and the lowest peak value in the incoming heat flux (q_{max} = 2.3 W/m^2). The peak occurs in the early morning of the following day (τ_{qmax} = 3:00), thanks to the combined effect of thermal mass and high level of thermal insulation that notably delays the incoming heat flux (see Fig. 10a).

The addition of a DWC hydroponic module to the lightweight roof (*LW_HR*) and to the lightweight concrete roof (*HB_HR*) notably dampens the amplitude of fluctuations and strongly decreases the peaks compared to the corresponding bare scenarios (*LW, HB*). The heat flux is now outgoing all day long in the summer week, even during the peak sunny hours, thanks to the simultaneous effect of shading and thermal mass provided by the water tray (see Fig. 10b). During the daily hours the hydroponic system almost completely decouples the indoor thermal environment from the external one. The hydroponic module remarkably delays the peak value, which is shifted from 13:00 to 5:00 of the next day for the lightweight roof (*LW_HR*) and from 21:00 to 5:00 for the *HB_HR* scenario.

The addition of the hydroponic module to the well-insulated lightweight concrete roof (*INS_HB_HR*) further reduces the fluctuations of the incoming heat flux and delays the peak with respect to the bare roof

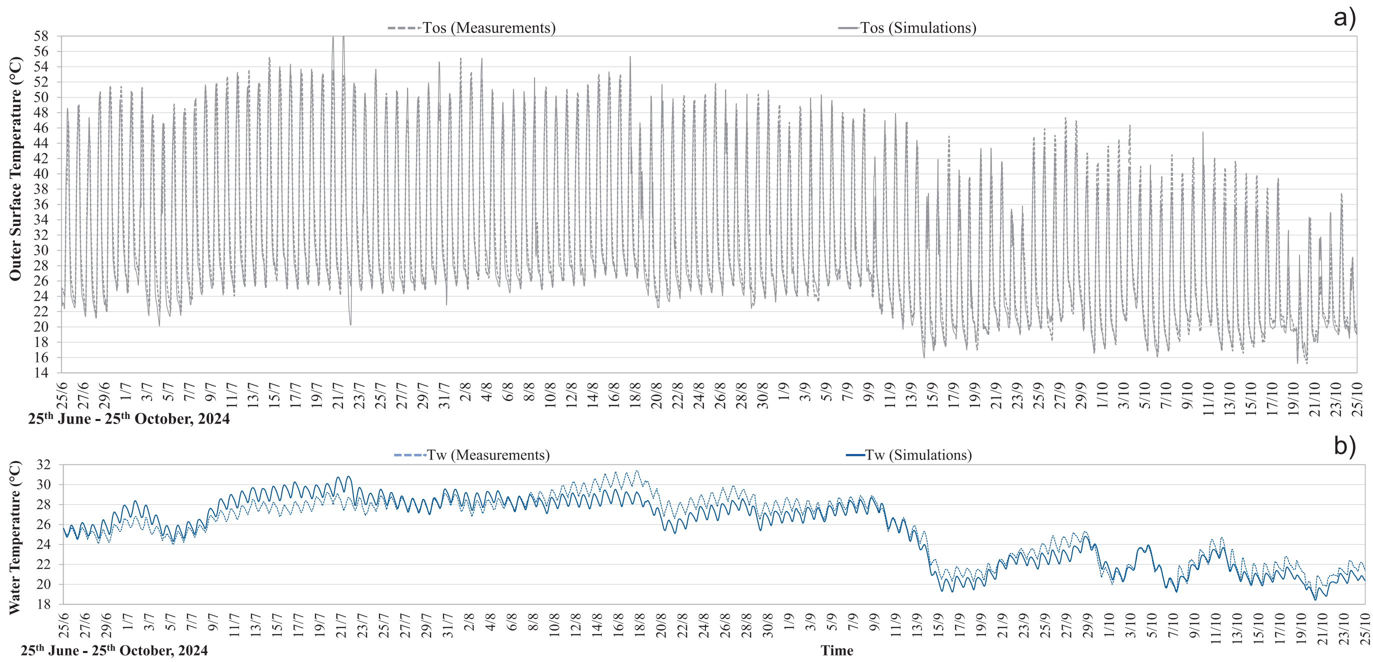

Fig. 6. Comparison between experimental measurements and predicted data from 25th June to 25th October. a) Outer surface Temperature (T_{os}) of the bare roof (BR); b) Water temperature (T_w) in the hydroponic roof module (HR).

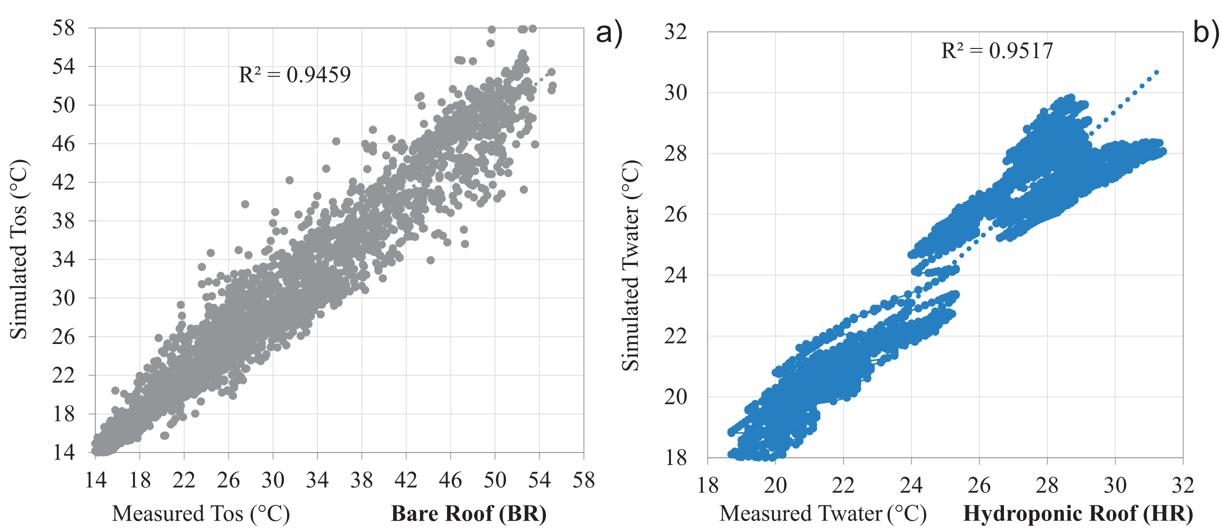

Fig. 7. Linear regression and coefficient of determination (R^2) for the external surface temperature of the bare roof (BR, on the left) and water temperature of the Hydroponic roof (HR, on the right).

configuration (*INS_HB*). The reduction in the peak values compared to the *INS_HB* scenario is lower if compared to that of other investigated roof scenarios (*LW_HR*, *HB_HR*) because the roof is already well-insulated.

On the other hand, the trends during the winter week in the bare roof configurations (Fig. 11a) show that the widest fluctuations are achieved by the lightweight concrete roof without thermal insulation (*HB*). Indeed, q varies from a minimum of –12.2 W/m^2 to a maximum of 8.8 W/m^2. The *LW* configuration is characterized by lower fluctuations with respect to the *HB* scenario, whereas the *INS_HB* configuration shows the smallest daily fluctuations, in the range of -2 W/m^2 $\div$ $+2$ W/m^2.

The hydroponic module thus confirms its greater effectiveness in improving indoor thermal conditions in the presence of an uninsulated lightweight concrete roof also during a typical winter week. Indeed, the peak of q is reduced until to 0.7 W/m^2 in the *HB_HR* configurations.

A remarkable reduction is also achieved by the lightweight configuration with hydroponic module (*LW_HR*). On the contrary, the effect of the hydroponic module is less evident in the configuration with a good insulation level (*INS_HB_HR*) with respect to the other hydroponic roof configurations (see Fig. 11b).

Overall, the results reveal the ability of the DWC hydroponic roof module to dampen the amplitude of the fluctuation of the incoming heat flux thanks to the thermal mass provided by the water tank in all analysed scenarios.

Finally, the thermal performance of the DWC hydroponic roof has been assessed also in terms of annual energy demand for space cooling (CE) and heating (HE). Fig. 12 depicts the predicted energy demand, as well as the energy savings compared to the corresponding bare roof (BR) configurations, split for space cooling (Fig. 12a) and heating (Fig. 12b).

The results of the simulations show that the configuration *HB*

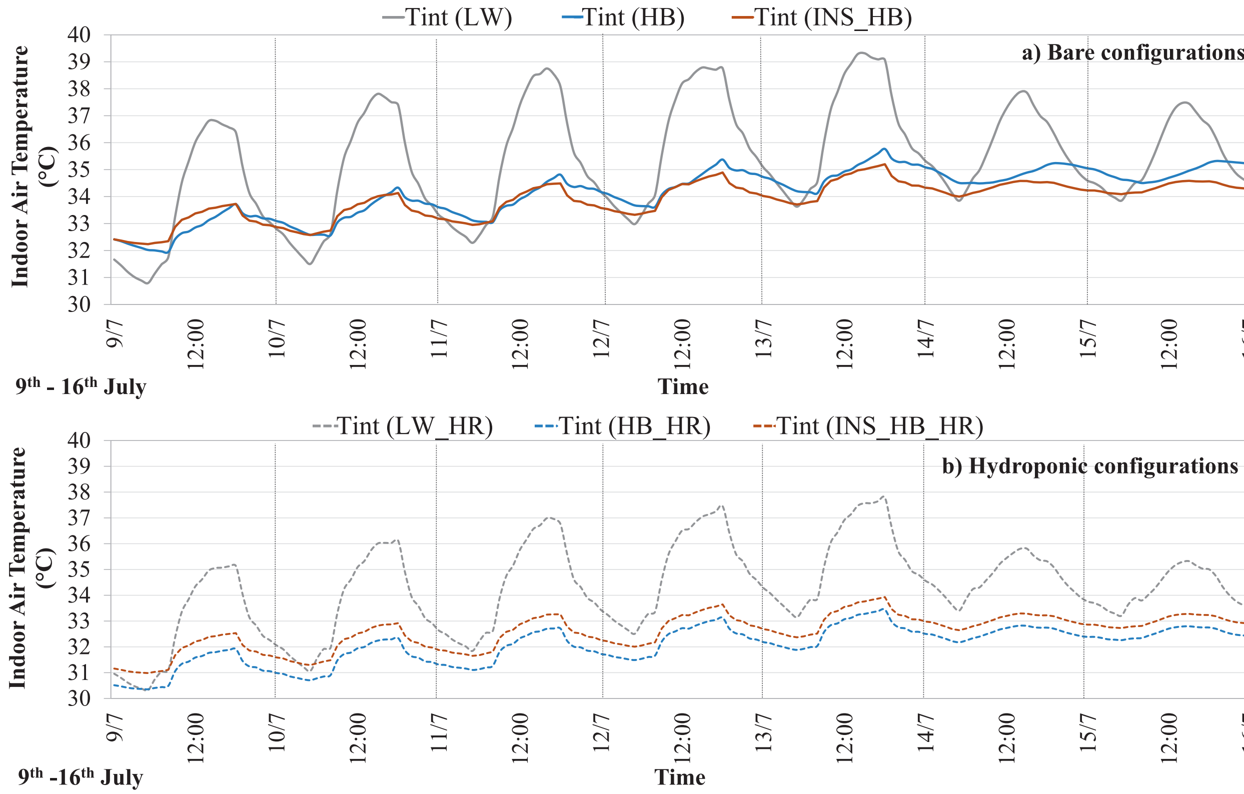

Fig. 8. Simulated daily profile of indoor air temperature (T_{int}) from 9th to 16th July. a) Bare roof configurations (BR); b) Hydroponic roof configurations (HR).

a) Bare roof configurations (BR); b) Hydroponic roof configurations (HR).

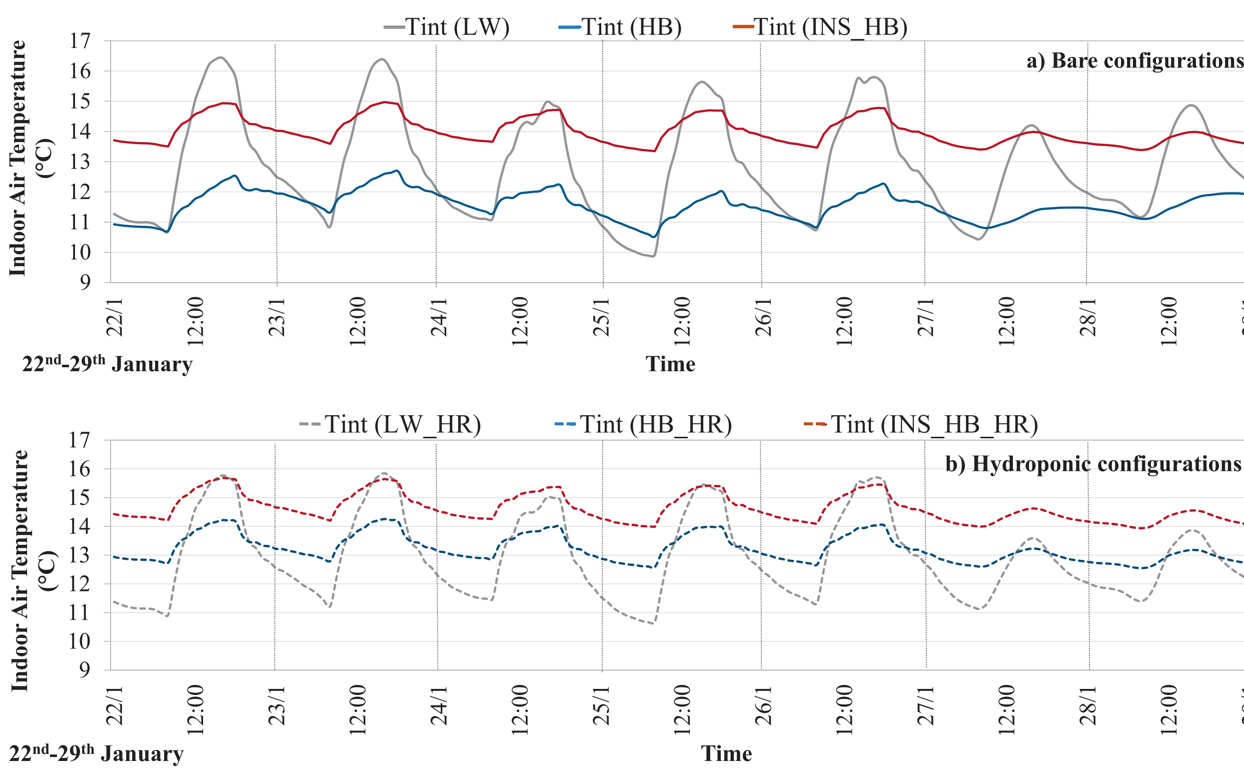

Fig. 9. Simulated daily profile of indoor air temperature (T_{int}) from 22nd to 29th January. a) Bare roof configurations (BR); b) Hydroponic roof configurations (HR).

Table 7
Results regarding the internal air temperature (T_{int}) on a typical summer day (13rd July) and winter day (25th January).

	Configurations	Summer day (13 July)			Winter day (25January)		
		$T_{int,max}$ (°C)	$T_{int,min}$ (°C)	$\Delta T_{int,peak}$ (°C)	$T_{int,max}$ (°C)	$T_{int,min}$ (°C)	$\Delta T_{int,peak,}$ (°C)
Bare roof configurations (BR)	*LW*	39.4	33.6	–	15.6	9.9	–
	HB	35.8	34.1	–	12.0	10.5	
	INS_HB	35.2	33.7	–	14.7	13.3	–
Hydroponic configurations (HR)	*LW_HR*	37.7	33.1	1.7	15.1	10.7	0.5
	HB_HR	33.4	31.9	2.4	14.1	12.7	−2.1
	INS_HB_HR	33.9	32.3	1.3	15.7	14.1	−1.0

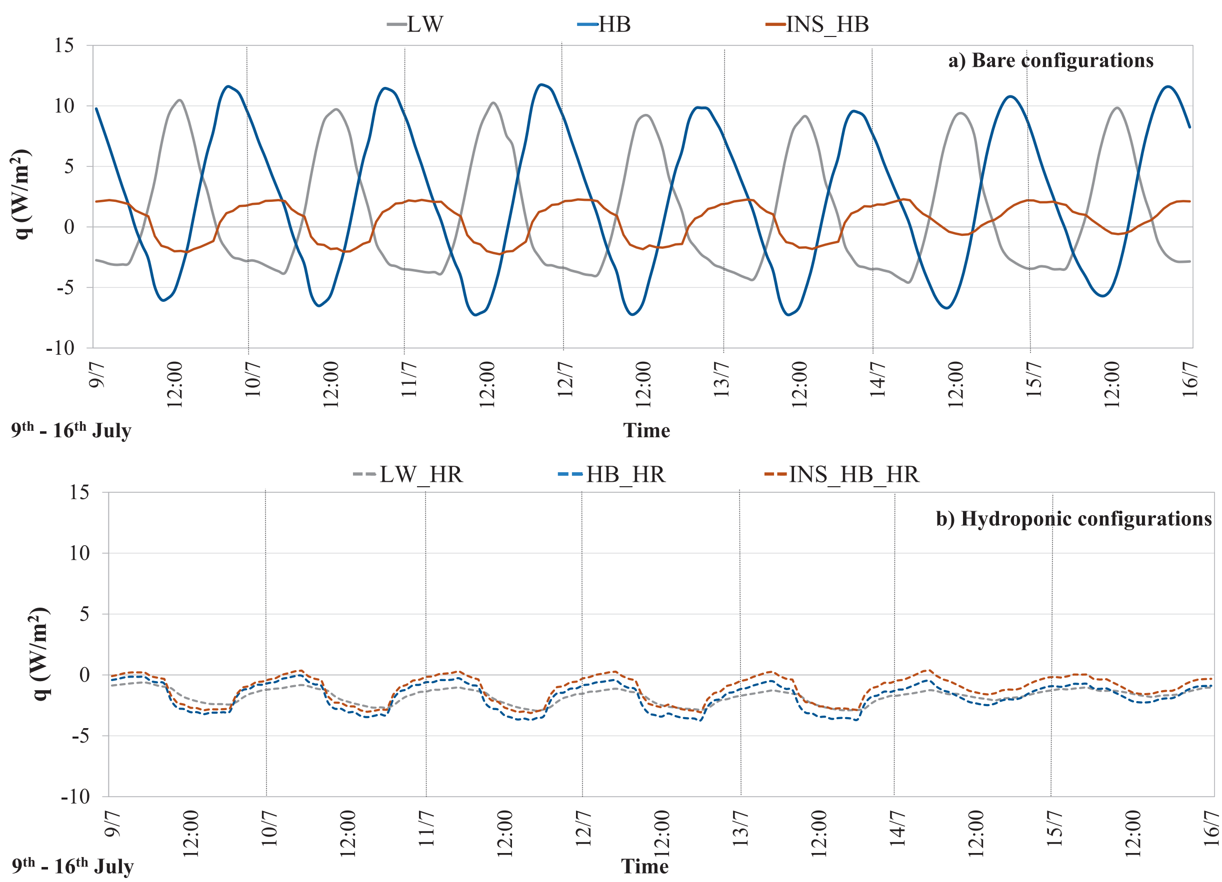

Fig. 10. Simulated daily profile of the heat flux from the roof surface to the indoors during the summer week (9th – 16th July) a) Bare roof configurations; b) Hydroponic roof configurations.

(lightweight concrete roof and walls made by hollow clay blocks) has the highest energy demand for space cooling (CE = 32.1 kWh/(m^2·y)). On the other hand, the insulated lightweight scenario (*LW*) and the scenario with a high level of thermal insulation (*INS_HB*) present CE values of 26.0 and 22.7 kWh/(m^2·y), respectively. In the presence of a DWC hydroponic module, a reduction higher than 20% in the energy demand for space cooling has been achieved in all the investigated scenarios: this result stems from the buffering effect and insulating capacity of the hydroponic system that dampens and delays the entering heat flux. It is worth highlighting that the addition of a DWC hydroponic module has the highest impact in the energy demand for cooling in the uninsulated roof and walls configurations (*HB* scenario). Indeed, the *HB_HR* configuration allows reducing the CE by about 47% with respect to the bare configuration (*HB*).

These findings are quite similar to those reported by Ibrahim et al. [20] for a hydroponic system with 15 cm water depth simulated in Alexandria (Egypt), where cooling energy savings amounted to 15% for a slightly-insulated concrete roof structure.

For the *LW_HR* and *HB_HR* configurations, instead, the predicted energy savings for space cooling (ES_C) are of 29% and 21%, respectively. As it is possible to see from Fig. 12a, the inclusion of a Hydroponic roof module in an uninsulated roof (*HB_HR*) reduces the energy demand for space cooling more than in the case of the thermal insulated bare roof (*INS_HB*). This occurs because the internal air temperature in the *INS_HB* configuration is always higher than that of the uninsulated lightweight concrete roof with hydroponic module *HB_HR*. Therefore, in presence of the Hydroponic module, there would be no need to add thermal insulation to the roof to achieve relevant energy savings for space cooling.

As regards the heating energy demand (HE), the highest energy savings are achieved by the *HB_HR* configuration (around 51%), whereas the insulated roof configurations (*LW_HR, INS_HB_HR*) have ES_H lower than 17% (see Fig. 12b).

Finally, if looking at the global energy demand (cooling and heating) it appears that the uninsulated hollow block roof configuration (*HB*) shows the highest energy demand (57.4 kWh/(m^2·y)), whereas the insulated lightweight configuration (*LW*) and hollow clay blocks roof with thermal insulation (*INS_HB*) have comparable values (33.1 kWh/(m^2·y) and 32.1 kWh/(m^2·y)). The addition of a hydroponic roof module

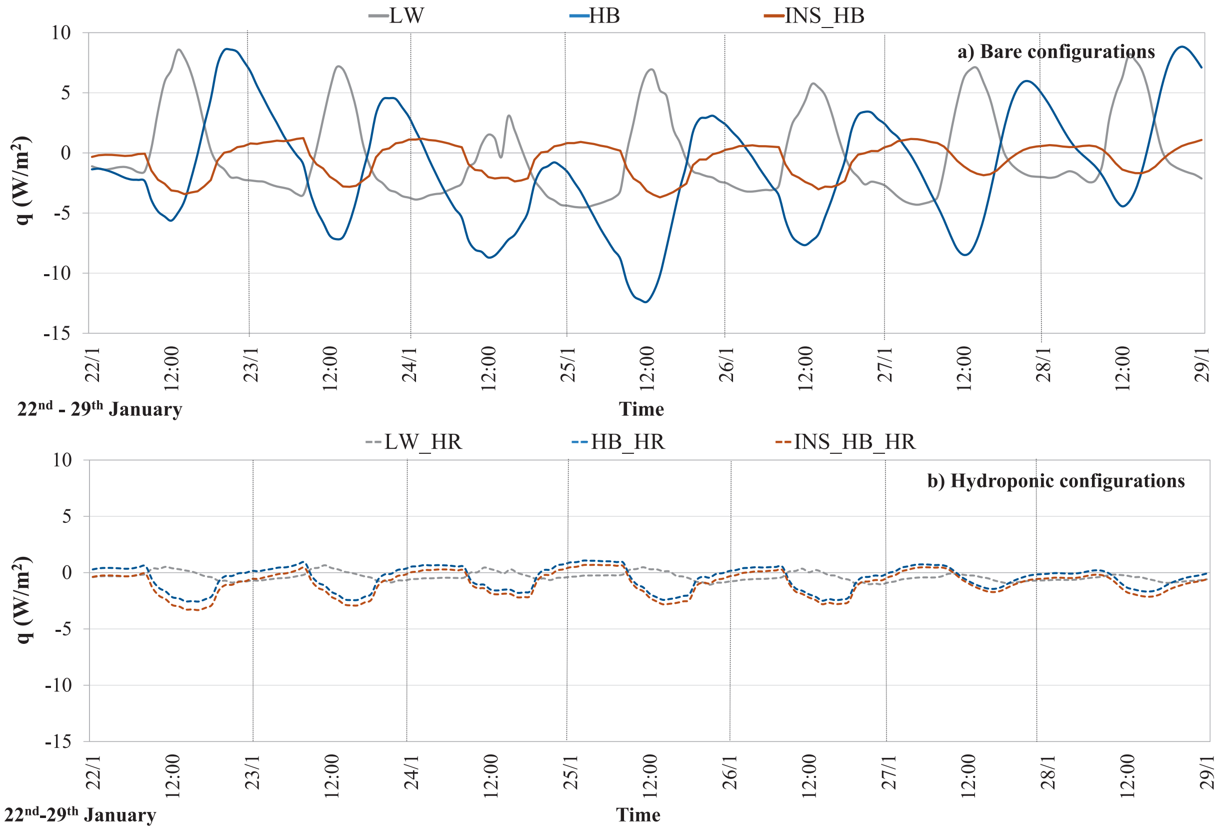

Fig. 11. Simulated daily profile of the heat flux from the roof surface to the indoors during the winter week (22nd – 29th January) a) Bare roof configurations; b) Hydroponic roof configurations.

Table 8
Results regarding the heat flux (q) in the bare configurations (BR) and with hydroponic roof (HR) during the summer week (9th – 16th July) and the winter week (22nd –29th January).

	Configurations	Summer week (9th-16th July)		Winter week (22nd-29th January)	
		q_{max} (W/m²)	τ_{qmax}	q_{max} (W/m²)	τ_{qmax}
Bare configurations (BR)	*LW*	10.4	13:00	8.6	13:00
	HB	11.7	21:00	8.8	21.00
	INS_HB	2.3	3.00	1.2	3:00
Hydroponic configurations (HR)	*LW_HR*	−0.6	5:00	0.7	12:00
	HB_HR	−0.1	5:00	1.1	5:00
	INS_HB_HR	0.4	5:00	0.7	6:00

provides the highest impact on the uninsulated lightweight concrete roof configuration (*HB*), where a total energy saving of about 48% can be achieved. The thermal insulated configurations with hydroponic module (*LW_HR*, *INS_HB_HR*) have potential total energy savings of 26% and 18%, in order. These savings are lower in magnitude than those achieved by the uninsulated roof configurations, but still worth of interest because of the benefits in terms of better indoor thermal conditions.

3.4. Sensitivity analysis

The effects of different water depths in the tray were appraised for the investigated roof typologies by varying the initial value of 30 cm to a lower (20 cm) and a higher (40 cm) one, respectively. The difference between the peak values of indoor air temperature (ΔT_{peak}) in both the summer day (13rd July) and the winter day (25th January), along with the annual energy savings for heating demand (HEs) and cooling demand (CEs), were calculated as a difference between the bare roof configurations and the corresponding ones embedding the hydroponic module.

Table 9 reports the thermal features (thickness, thermal transmittance and surface mass) of the investigated roof scenarios and the relative simulation results of the sensitivity analysis to the water depth.

The simulation results revealed that using a water depth of 20 cm allows achieving the highest reduction in the peak of indoor air temperature (ΔT_{peak}) in the summer day in all the investigated roof typologies, especially for the uninsulated concrete slab with hollow clay blocks (*HB_HR_I*) and lightweight prefabricated roof (*LW_HR_I*), which show a reduction by 2.4 °C and 1.9 °C, respectively.

In the winter, the hydroponic module with a water depth of 20 cm on the uninsulated concrete slab increases the peak of indoor air temperature by 1.6 °C compared to the bare roof configuration (*HB*). On the contrary, the presence of hydroponic module leads to a reduction by 0.8 °C under *LW* configuration. On the other hand, the indoor air temperature keeps almost the same when increasing the water depth from 30 cm to 40 cm in all investigated roof typologies.

The DWC hydroponic roof with a water depth of 20 cm appears the best performing configuration also in terms of energy demand: in fact, the uninsulated concrete slab configuration (*HB_HR_I*) showed the highest energy savings for cooling (CEs = 48%) and heating demand (HEs = 46%). A notable reduction in the cooling energy demand (CE_S = 29.4%) is predicted also for the lightweight prefabricated roof (*LW*). Further increasing the water depth in the hydroponic tray contributed to increase the energy savings for space heating (HEs), while no appreciable improvements were predicted in the cooling performance: this result stems from the increased thermal resistance of the roof, which helps reducing the heat losses.

Considering these results, further simulations regarding the effects of

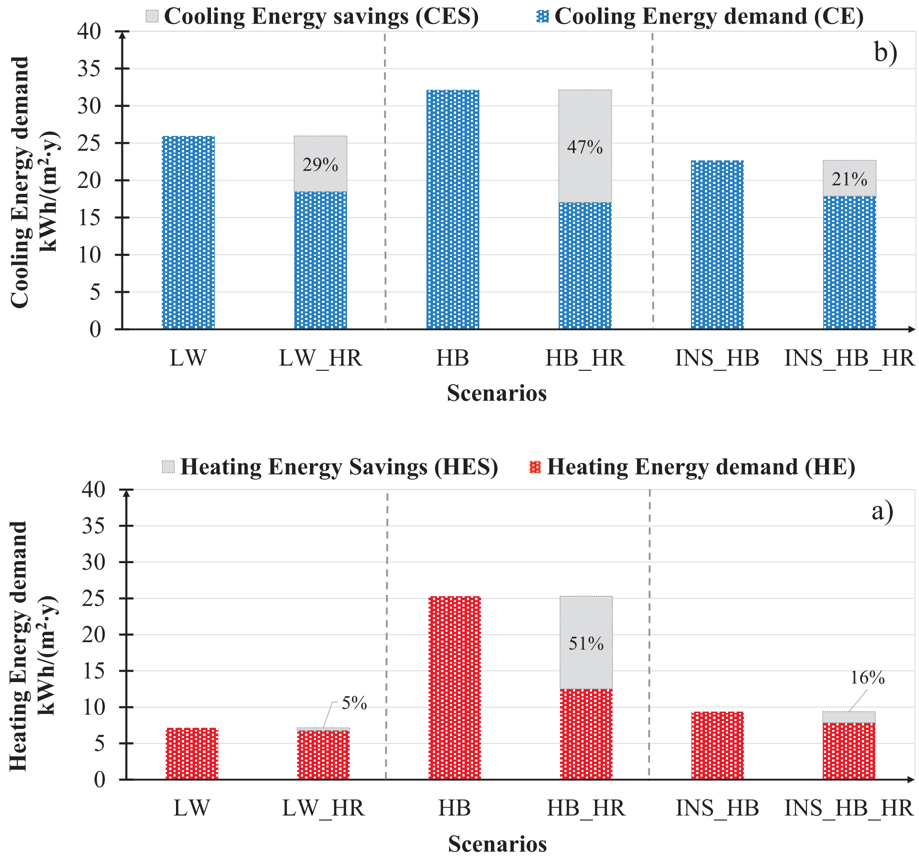

Fig. 12. Thermal energy demand per unit of net floor area: a) Cooling; b) Heating.

Table 9
Main thermal features and simulation outcomes of the sensitivity analysis to the water depth.

Investigated roof typology	Water depth (cm)	Roof configuration	t cm	U $W/(m^2{\cdot}K)$	SM kg/m^2	ΔT_{peak}(°C) Summer day (13rd July)	Winter day (25th January)	CE_S %	HEs %
LW	–	LW (bare roof)	8	0.52	15	–	–	–	–
	20	LW_HR_I	42	0.23	213	1.9	0.8	29.4	3.1
	30	LW_HR_II	52	0.22	313	1.7	0.5	29.1	5.8
	40	LW_HR_III	62	0.21	413	1.7	0.4	28.9	12.5
HB	–	HB (bare roof)	31	1.57	367	–	–	–	–
	20	HB_HR_I	65	0.32	576	2.4	−1.6	48.0	46.0
	30	HB_HR_II	75	0.31	671	2.3	−2.1	47.3	51.2
	40	HB_HR_III	85	0.30	722	2.3	−2.5	47.0	56.2
INS_HB	–	INS_HB (bare roof)	39	0.34	422	–	–	–	–
	20	INS_HB_HR_I	73	0.20	602	1.5	−0.5	20.7	9.2
	30	INS_HB_HR_II	83	0.19	705	1.3	−1.0	20.6	16.4
	40	INS_HB_HR_III	93	0.17	780	1.3	−1.2	20.5	22.5

different vegetation fraction cover (X_{veg}) were performed only for the hydroponic roof configurations with water depth of 20 cm (*LW_HR_I, HB_HR_I*, *INS_HB_HR_I*). In particular, the reduction in the peak of internal air temperature and annual energy savings for cooling and heating were appraised for $X_{veg} = 0.30$, 0.60, and 0.90, respectively, and are summarized in Table 10.

The parametric analysis shows that the increase of the vegetation fraction contributes to reducing the peak values of indoor air temperature in all the investigated roof typologies, both in the summer and winter days. This result is substantially due to the increase of the shading effect of the vegetation, which reduces the incoming heat flux from the incident solar radiation. In the summer, the reduction in the peak values of indoor air temperature is a positive outcome, as it improves the indoor thermal conditions; on the contrary, the same increase slightly worsens the thermal conditions in the winter (see Table 10).

In terms of energy performance, the annual energy demand for space heating raises by increasing the vegetation fraction cover in all the roof typologies, as demonstrated by the slight reduction of the annual energy savings for heating demand (HEs). On the contrary, the annual energy savings for cooling demand (CEs) are slightly increased in all investigated roof scenarios by varying the X_{veg} values from 0.3 to 0.9. However, increasing the X_{veg} value from 0.60 to 0.90 gave negligible benefits in all roof scenarios. In light of these results, the adoption of a vegetation fraction below 60% can already ensure good thermal and energy performances.

In the end, the hydroponic module configuration with a water tray depth of 20 cm and with a vegetation fraction lower than 60% appears to be the best solution for all the investigated roof typologies, giving the real breakthrough both in terms of indoor thermal conditions and energy demand reduction for space cooling. The increase of the tray depth up to

Table 10
Main thermal features and simulation outcomes of the sensitivity analysis to the vegetation fraction cover.

Roof scenarios	X_{veg} (−)	Roof configurations	ΔT_{max} (°C) Summer day (13rd July)	Winter day (25th January)	CEs %	HEs %
LW (Bare roof)	–	–	–	–	–	–
LW_HR_I	0.3	$LW\_HR\_I_{03}$	1.8	0.6	29.5	3.1
	0.6	$LW\_HR\_I_{06}$	2.1	0.9	31.3	2.9
	0.9	$LW\_HR\_I_{09}$	2.3	1.0	32.5	2.8
HB (Bare roof)	–	–	–	–	–	–
HB_HR_I	0.3	$HB\_HR\_I_{03}$	2.3	−2.1	48.1	46.2
	0.6	$HB\_HR\_I_{06}$	2.6	−2.0	50.8	44.1
	0.9	$HB\_HR\_I_{09}$	2.8	−1.8	51.9	45.4
INS_HB (Bare roof)	–	–	–	–	–	–
	0.3	$INS\_HB\_HR\_I_{03}$	1.3	−0.6	20.7	9.2
INS_HB_HR_I	0.6	$INS\_HB\_HR\_I_{06}$	1.6	−0.5	22.6	8.8
	0.9	$INS\_HB\_HR\_I_{09}$	1.7	−0.4	23.3	8.5

30 or 40 cm did not lead to appreciable thermal benefits, while slightly worsening the thermal performance because the water mass tends to remain warmer in the hottest hours due to the increased thermal capacity of the roof. Moreover, it adds an unnecessary additional load to the roof structure, potentially undermining the applicability of the hydroponic roof to existing roof structures at least in Italy, where reinforced concrete slabs where typically designed to bear a structural overload of around 200 kg/m^2 [27].

4. Conclusions

The present paper investigated the effectiveness of a novel Deep Water Culture (DWC) Hydroponic roof module in improving the indoor thermal conditions in a sample office room during summer and winter periods, while also reducing the energy demand for space cooling and heating. To this aim, a prototype of hydroponic module based on the DWC technique was designed, installed and monitored on a conventional flat roof of an existing building at the University campus of Catania (Italy) in the context of FUD-OF-SITHY project – "Favor the Urban Development OF Sustainable Agriculture Through Hydroponics".

According to the experimental results, the hydroponic module stabilizes the water temperature in the tank between 24.0 °C and 29.0 °C with an amplitude of daily fluctuations lower than 2.0 °C in the hottest summer period (from 25th June to 20th July). The validation of an ad-hoc TRNSYS model revealed a good agreement and an excellent correlation with the experimental evidence (MAE = 1.75 °C, R^2 = 0.94) for both the external surface temperature of the conventional bare roof and the water temperature in the Hydroponic module (MAE = 1.14 °C, R^2 = 0.95). Thus, the validated model was used to simulate different roof configurations and appraise the indoor thermal conditions during a typical summer and winter week, while also evaluating the heat flux exchanged through the roof and the resulting energy demand for space heating and cooling. Results revealed that the hydroponic roof module enhances the internal thermal conditions in all the investigated roof scenarios thanks to the additional thermal mass brought about by the water tank that allows stabilizing the indoor air temperature, while reducing and delaying the peak of the incoming heat flux. In particular, the hydroponic module shows the best performances for the uninsulated roof configuration made by hollow clay blocks and lightweight concrete (*HB_HR*): in this case, the peak indoor air temperature is reduced by up to 2.4 °C and delayed from 9:00 pm to 5.00 am in a hot summer day. The swing of heat flux entering the building is significantly dampened too, so that the peak is reduced from 11.7 W/m^2 to almost zero and delayed from 9:00 pm to 5.00 am.

In terms of energy demand, the hydroponic configuration applied to an uninsulated roof (*HB_HR*) confirms the higher energy savings, which are of about 47% for space cooling and 51% for space heating. A sensitivity analysis has proved also that a water depth of 20 cm and a vegetation cover fraction lower than 60% appears to be the best solution for all the investigated roof typologies, representing a good trade-off between thermal and energy performance and the reduction of the additional load to the existing roof structure. Further numerical analyses are planned to find the optimal configurations of the hydroponic module prototype under different climates.

CRediT authorship contribution statement

V. Costanzo: Writing – review & editing, Writing – original draft, Validation, Supervision, Methodology, Investigation, Formal analysis, Conceptualization. **M. Detommaso:** Writing – original draft, Visualization, Software, Investigation, Formal analysis, Data curation. **G. Evola:** Writing – review & editing, Visualization, Supervision, Investigation. **F. Nocera:** Writing – review & editing, Supervision, Software, Resources, Project administration, Investigation, Funding acquisition, Conceptualization. **M. Mistretta:** Resources, Project administration, Funding acquisition, Conceptualization. **S. Longo:** Resources, Project administration, Investigation, Funding acquisition, Conceptualization.

Declaration of competing interest

The authors declare that they have no known competing financial interests or personal relationships that could have appeared to influence the work reported in this paper.

Acknowledgements

This research was made possible through the generous support of the FUD-OF-SITHY project - "Favor the Urban Development OF Sustainable Agriculture Through HYdroponics" - P2022F9HEW, funded under the National Recovery and Resilience Plan (PNRR) with the identifier CUP E53D23017150001, and of the PIA.CE.RI. 2024-2026 Linea 1 GREEN project (PI prof. F. Nocera). The authors would like also to thank the SECA laboratory for providing the re-search team with all the necessary instruments and software tools.

Data availability

Data will be made available on request.

References

[1] Global Status Report for Buildings and Construction, Towards a zero-emissions, efficient and resilient buildings and construction sector, United Nations Environment Programme, 2019. https//www.iea.org.

[2] H. L. Macintyre, C. Heaviside, J. Taylor, R. Picetti, P. Symonds, X.M. Cai, S. Vardoulakis, Assessing urban population vulnerability and environmental risks across an urban area during heatwaves – Implications for health protection, Science of the Total Environment. 610 (2018) 678-690. https://doi: 10.1016/j.scitotenv.2017.08.062.

[3] K. Szulecki, D.H. Claes, Towards Decarbonization: Understanding EU Energy Governance, Politics and Governance. 7(1) (2019) 1–5. https://doi: 10.17645/pag.v7i1.2029.
[4] K. Perini, F. Bazzocchi, L. Croci, A. Magliocco, E. Cattaneo, The use of vertical greening systems to reduce the energy demand for air conditioning, Field Monitoring in Mediterranean Climate, Energy and Buildings 143 (2017) 35–42, https://doi.org/10.1016/j.enbuild.2017.03.036.
[5] R.C. Feitosa, S.J. Wilkinson, Attenuating heat stress through green roof and green wall retrofit, Build. Environ. 140 (2018) 11–22, https://doi.org/10.1016/j.buildenv.2018.05.034.
[6] S. Seyam, The impact of greenery systems on building energy: Systematic review, Journal of Building Engineering. 26 (2019) 100887, https://doi.org/10.1016/j.jobe.2019.100887.
[7] F. Nocera, V. Costanzo, M. Detommaso, G. Evola, Assessing the impact of vertical greenery systems on the thermal performance of walls in Mediterranean climates, Energies 17 (2024) 5090, https://doi.org/10.3390/en17205090.
[8] H. Akbari, C. Cartalis, D. Kolokotsa, A. Muscio, A.L. Pisello, F. Rossi, M. Santamouris, A. Synnefa, N. Wong, M. Zinzi, Local climate change and urban heat island mitigation techniques – the state of the art, Journal Civil Engineering and Management. 22 (1) (2016) 1–16, https://doi.org/10.3846/13923730.2015.1111934.
[9] R. Rapisarda, F. Nocera, V. Costanzo, G. Sciuto, R. Caponetto, Hydroponic green roof systems as an alternative to traditional pond and green roofs: a literature review, Energies 15 (2022) 2190, https://doi.org/10.3390/en15062190.
[10] D. Qiu, H. Peng, T. Li, Y. Qi, Application of stabilized sludge to extensive green roofs in Shanghai: Feasibility and nitrogen leaching control, Science of Total Environment. 732 (2020) 138898. doi: 10.1016/j.scitotenv.2020.138898.
[11] D.J. Sailor, D. Hutchinson, L. Bokovoy, Thermal property measurements for ecoroof soils common in the western U.S, Energ. Buildings 40 (2008) 1246–1251, https://doi.org/10.1016/j.enbuild.2007.11.004.
[12] J. Muñoz-Liesa, S. Toboso-Chavero, A. Mendoza Beltran, E. Cuerva, E. Gallo, S. Gassó-Domingo, A. Josa, Building-integrated agriculture: are we shifting environmental impacts? an environmental assessment and structural improvement of urban greenhouses, Resour. Conserv. Recycl. 169 (2021) 105526, https://doi.org/10.1016/j.resconrec.2021.105526.
[13] D. Gould, T. Caplow, Building-integrated agriculture: a new approach to food production, Metropolitan Sustainability Understanding and Improving the Urban Environment Woodhead Publishing Series in Energy. (2012) 147-170. https://doi.org/10.1533/9780857096463.2.147.
[14] M. D'Ostuni, L. Zaffi, E. Appolloni, F. Orsini, Understanding the complexities of Building-Integrated Agriculture. can food shape the future built environment? Futures 144 (2022) 103061 https://doi.org/10.1016/j.futures.2022.103061.
[15] N.C. Barman, M.M. Hasan, M.R. Islam, N.A. Banu, A review on present status and future prospective of hydroponics technique, Plant Environment Development. 5 (2) (2016) 1–7.
[16] M. Majid, J.N. Khan, Q.M.A. Shah, K.Z. Masoodi, B. Afroza, S. Parvaze, Evaluation of hydroponic systems for the cultivation of Lettuce (*Lactuca sativa* L., var. Longifolia) and comparison with protected soil-based cultivation, Agric Water Manag 245 (2021) 106572, https://doi.org/10.1016/j.agwat.2020.106572.
[17] Y. Huang, C. Chen, Y. Tsai, Reduction of temperatures and temperature fluctuations by hydroponic green roofs in a subtropical urban climate, Energy and Building. 129 (2016) 174–185, https://doi.org/10.1016/j.enbuild.2016.07.023.
[18] E. Alexandri , P. Jones , Ponds, Green Roofs, Pergolas and High Albedo Materials; Which Cooling Technique for Urban Spaces? In Proceedings of the PLEA2006—The 23rd Conference on Passive and Low Energy Architecture, Geneva, Switzerland, 6–8 September 2006.
[19] Y. Tanaka, S. Kawashima, T. Hama, L.F. Sanchez Sastre, K. Nakamura, Y. Okumoto, Mitigation of heating of an urban building rooftop during hot summer by a hydroponic rice system, Build. Environ. 96 (2016) 217–227, https://doi.org/10.1016/j.buildenv.2015.11.025.
[20] A.M. Ibrahim, W.F. Omar, M.A. Mahdy, The effect of Hydroponics Planted Roof on the thermal Performance of Indoor Residential Spaces in Egypt, Scientific Journal of the Faculty of Fine Arts. 10 (2) (2022).
[21] UNI EN ISO 10456:2008. Building materials and products - Hygrothermal properties - Tabulated design values and procedures for determining declared and design thermal values.
[22] UNI 10351:2021. Building materials - Thermo-hygrometric proprieties - Procedure for determining the design values.
[23] UNI EN 6946:2018. Building components and building elements - Thermal resistance and thermal transmittance - Calculation methods.
[24] V. Costanzo, G. Evola, M. Infantone, L. Marletta, Updated typical Weather Years for the Energy simulation of buildings in Mediterranean climate. a case study for Sicily, Energies 13 (16) (2020) 4115.
[25] J. Hong, Optimal design of green roofs: Mathematical model and experimental evidence, Theses and Dissertations. 1825 (2018).
[26] D.M. Gates, Biophysical ecology, Dover Publications, New York, 2003.
[27] Italian National Technical Standards for Construction (NTC 2018). Infrastructure and Transport Minister 17 January 2018. Update of the technical rules for constructions.